motely (*18*). This substantial neutral source from Enceladus may go some way toward answering one of the outstanding questions regarding our understanding of Saturn's magnetosphere: What is the missing source of the large densities of water and its derivatives that are observed?

References and Notes

1. M. K. Dougherty *et al.*, *Space Sci. Rev.* **114**, 331 (2004).
2. J. R. Spencer *et al.*, *Science* **311**, 1401 (2006).
3. R. H. Brown *et al.*, *Science* **311**, 1425 (2006).
4. C. C. Porco *et al.*, *Science* **311**, 1393 (2006).
5. C. J. Hansen *et al.*, *Science* **311**, 1422 (2006).
6. J. H. Waite Jr. *et al.*, *Science* **311**, 1419 (2006).
7. ENIS is defined with *X* in the direction of corotational flow; *Y* is positive toward Saturn and *Z* is along Saturn's spin axis.
8. An Enceladus radius is defined as R_E = 252.1 km.
9. S. D. Drell, H. M. Foley, M. A. Ruderman, *J. Geophys. Res.* **70**, 3131 (1965).
10. F. M. Neubauer, *J. Geophys. Res.* **85**, 1171 (1980).
11. J. W. Belcher, *Science* **238**, 170 (1987).
12. M. G. Kivelson *et al.*, *J. Geophys. Res.* **106**, 26121 (2001).
13. J. Saur, D. F. Strobel, *Astrophys. J.* **620**, L115 (2005).
14. B. A. Smith *et al.*, *Science* **215**, 504 (1982).
15. A Saturn radius is defined as R_S = 60,268 km.
16. E. C. Sittler *et al.*, *J. Geophys. Res.* **109**, A01214 (2004).
17. D. E. Huddleston, R. J. Strangeway, J. Warnecke, C. T. Russell, M. G. Kivelson, *J. Geophys. Res.* **103**, 19887 (1998).
18. L. W. Esposito *et al.*, *Science* **307**, 1251 (2005); published online 16 December 2004 (10.1126/science.1105606).

5 October 2005; accepted 11 January 2006
10.1126/science.1120985

REPORT

The Interaction of the Atmosphere of Enceladus with Saturn's Plasma

R. L. Tokar,[1]* R. E. Johnson,[2] T. W. Hill,[3] D. H. Pontius,[4] W. S. Kurth,[5] F. J. Crary,[6] D. T. Young,[6] M. F. Thomsen,[1] D. B. Reisenfeld,[7] A. J. Coates,[8] G. R. Lewis,[8] E. C. Sittler,[9] D. A. Gurnett[5]

During the 14 July 2005 encounter of Cassini with Enceladus, the Cassini Plasma Spectrometer measured strong deflections in the corotating ion flow, commencing at least 27 Enceladus radii (27 × 252.1 kilometers) from Enceladus. The Cassini Radio and Plasma Wave Science instrument inferred little plasma density increase near Enceladus. These data are consistent with ion formation via charge exchange and pickup by Saturn's magnetic field. The charge exchange occurs between neutrals in the Enceladus atmosphere and corotating ions in Saturn's inner magnetosphere. Pickup ions are observed near Enceladus, and a total mass loading rate of about 100 kilograms per second (3×10^{27} H_2O molecules per second) is inferred.

Enceladus sits in an OH cloud, or torus, around Saturn that was originally detected by the Hubble Space Telescope (*1*). This cloud extends from about 3 to 8 Saturn radii [1 R_S (Saturn's radius) = 60,268 km] with maximum concentration (~10^3 cm^{-3}) inferred near the orbit of Enceladus (3.95 R_S). The OH cloud is produced by dissociation of H_2O, and although the peak concentration suggested that the largest source of water molecules was in the region near the orbit of Enceladus, the nature of this source was unknown. Models indicate that the source region near 4 R_S must provide ~80% of the total OH source, estimated to be ~0.4×10^{28} to 1×10^{28} H_2O molecules s^{-1} (*2*, *3*).

On 14 July 2005, the Cassini spacecraft passed within 168.2 km of Enceladus, through the cloud of neutrals and plasma (Fig. 1). The orbital speed of Enceladus is 12.6 km s^{-1}, whereas the thermal plasma corotates with Saturn at 39 km s^{-1} near Enceladus. Thus, the corotating plasma overtakes Enceladus, forming a corotational wake in the positive azimuthal direction at a speed of 26.4 km s^{-1}. Cassini passed upstream of this wake (Fig. 1B). A strong enhancement in the flux of plasma ions was detected by the Cassini Plasma Spectrometer (CAPS) (*4*) in two time intervals (Fig. 1) between t_1 = 19:41 UT and t_2 = 19:46 UT and between t_3 = 20:04 UT and t_4 = 20:26 UT.

Another Cassini instrument, the Radio and Plasma Wave Science (RPWS) instrument (*5*), measured electric field fluctuations as a function of frequency and time during the Enceladus encounter (Fig. 2). We consider first the RPWS data and then return to the CAPS data. RPWS provides an estimate of the total electron density, N_e, at Cassini from the measured frequency of the upper hybrid resonance band (Fig. 2). This frequency is a known function of both the magnetic field strength (*6*) and the total electron density. The emission observed near the upper hybrid resonance frequency is complex, with a smoothly varying narrowband emission at low frequencies and a more sporadic broadband extension to higher frequencies (Fig. 2). We assume that the narrowband relative maximum in the peak near the bottom of this complex line is the upper hybrid band and that the broadband extension to higher frequencies is a thermal plasma effect. The upper hybrid band indicates that the total electron density, shown approximately by the right-hand scale, smoothly increases from about 45 cm^{-3} at 19:30 UT to about 70 cm^{-3} at 20:04 UT. There is a short period close to Enceladus when the narrowband emission is not identifiable, likely due to dust particles hitting the spacecraft. During this time, it is not possible for RPWS to precisely determine the electron density, although there does not appear to be evidence for a substantial increase in the density (>~20%) at closest approach.

The study uses electron spectrometer, ELS, and ion mass spectrometer, IMS, data from CAPS

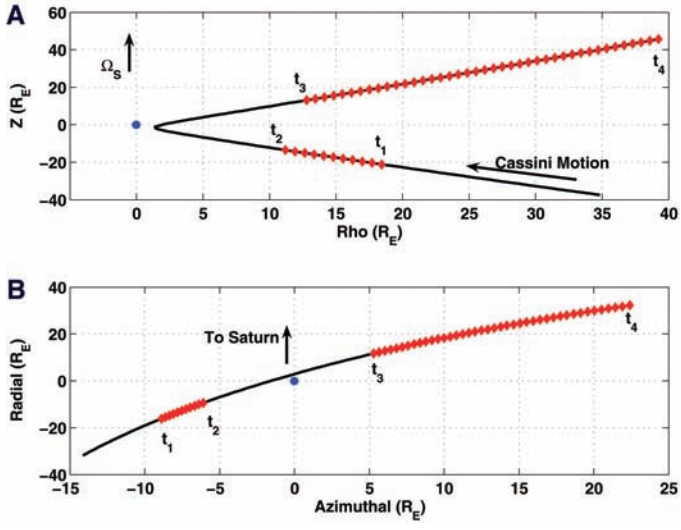

Fig. 1. Periods of CAPS-measured enhanced ion flux along the Cassini spacecraft trajectory during the close encounter of Enceladus on 14 July 2005. (**A**) An Enceladus-centered cylindrical coordinate system with the vertical axis in the direction of Saturn's spin axis and the horizontal axis the perpendicular distance from Enceladus (1 R_E = 252.1 km). (**B**) A projection into the equatorial plane with the radial coordinate positive toward Saturn and the azimuthal coordinate positive in the direction of corotation.

[1]Space Science and Applications, Los Alamos National Laboratory, Los Alamos, NM 87545, USA. [2]University of Virginia, Charlottesville, VA 22904, USA. [3]Rice University, Houston, TX 77251, USA. [4]Birmingham-Southern College, Birmingham, AL 35254, USA. [5]University of Iowa, Iowa City, IA 52242, USA. [6]Southwest Research Institute, San Antonio, TX 78228, USA. [7]University of Montana, Missoula, MT 59812, USA. [8]Mullard Space Science Laboratory, University College London, Holmbury St. Mary, Dorking, Surrey RH5 6NT, UK. [9]NASA Goddard Space Flight Center, Greenbelt, MD 20771, USA.

*To whom correspondence should be addressed. E-mail: rlt@lanl.gov

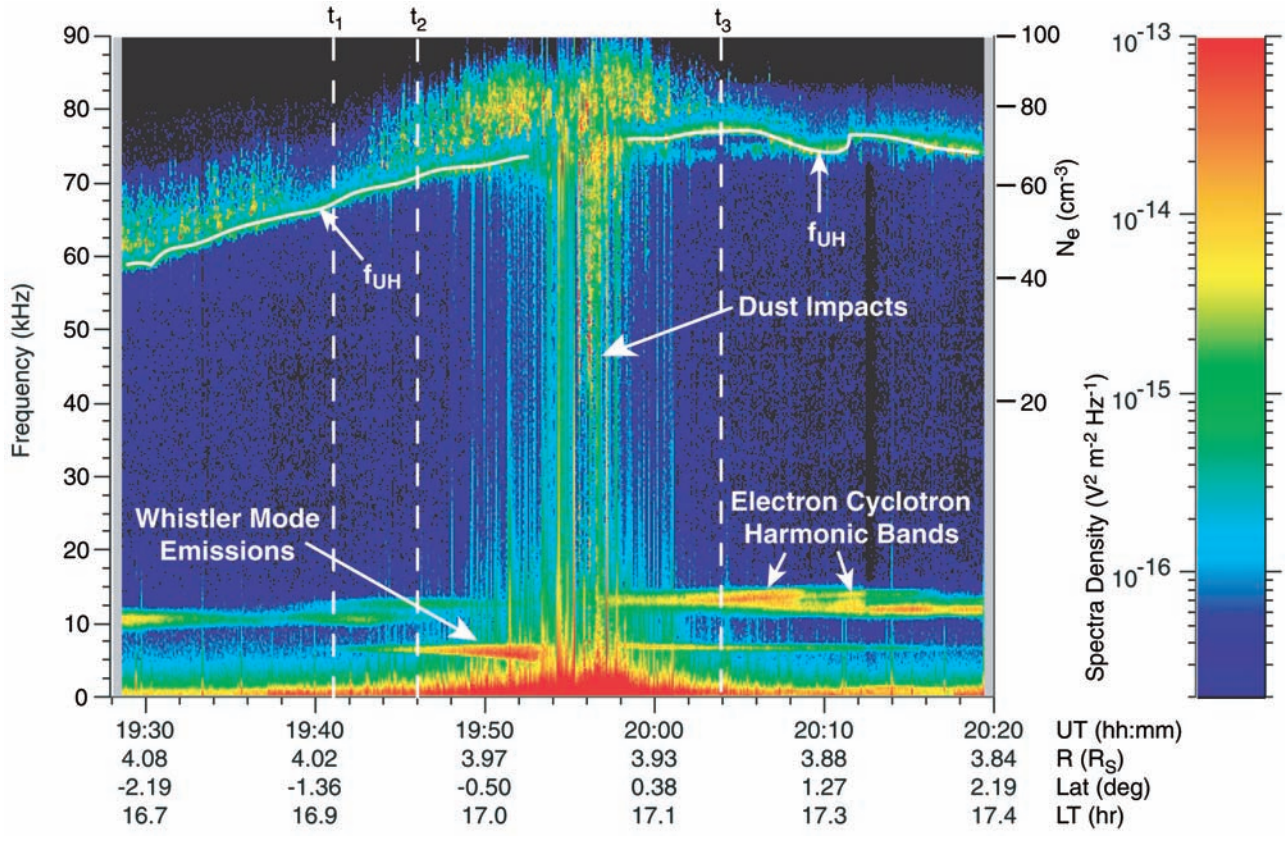

Fig. 2. Data from the Cassini RPWS instrument illustrating the electric field spectral density as a function of frequency and time on 14 July 2005. Upper hybrid, whistler mode, and electron cyclotron harmonic emissions are measured by RPWS, as is common in Saturn's inner magnetosphere. Closest approach to Enceladus occurs at 19:55 UT. The upper hybrid emission (f_{UH}) is a known function of the total electron density and magnetic field strength, yielding the electron density denoted in the upper right. LT is local time.

(*4*), with the penetrating radiation background removed (Fig. 3). Looking first at the electron counting rate as a function of energy and time, summed over the ELS field of view and uncorrected for spacecraft potential (Fig. 3A), two electron populations are visible: a "cold" (~2 to 3 eV) population with peak counts near A and a "hot" (~20 eV) population with peak counts near B. During the encounter with Enceladus, the spacecraft potential is less than the ELS minimum energy, making electron density and temperature extraction difficult. However, constraining the ELS data with the RPWS total electron density (Fig. 2), the spacecraft potential is ~–2 V, and the densities and the temperatures of cold and hot electron components are N_c = 70.3 cm^{-3} and T_c = 1.35 eV and N_h = 0.2 cm^{-3} and T_h = 12.5 eV, respectively. During the time interval from 19:30 to 20:30 UT, N_c and T_c vary by ~40% and ~20% respectively.

Next we consider the IMS ion counting rate as a function of energy and time (Fig. 3B). Although enhanced ion flux is observed throughout the encounter, a slowing and deflection of the ion flow velocity is observed when CAPS viewing is favorable, before closest approach (between 19:41 and 19:46 UT) and also after closest approach (between 20:14 and 20:26 UT). The ion composition can be obtained by IMS time-of-flight techniques (Fig. 3C) throughout the encounter, with water group ions O^+, OH^+, H_2O^+, and H_3O^+ detected.

To extract ion plasma moments, we used a forward model of IMS with the ions assumed to be O^+ and with phase space density a convected isotropic maxwellian. The free parameters in the model are ion temperature and two components of the ion flow velocity (radial and azimuthal). The ion temperature obtained from this procedure is ~35 eV away from Enceladus (at 19:41 and 20:26 UT) and decreases to ~15 eV closer to Enceladus (at 19:46 UT). The temperature away from Enceladus is consistent with previous CAPS results (*7*); the temperature further in is a rough estimate given the assumption of a single ion component (O^+) with isotropic phase space density. The ion flow velocity is constrained to lie in Saturn's equatorial plane, and the total ion density is constrained to equal the RPWS total electron density (Fig. 2). In Fig. 4, the ion flow velocity (red vectors) is plotted on the Cassini trajectory (Fig. 1B). Also shown for reference is the ion flow velocity for rigid corotation and model flow streamlines discussed below. The measured flow is slowed and deflected from the corotation direction at least 27 Enceladus radii (R_E; 1 R_E = 252.1 km) from the moon (at the start of the inbound segment), and at a distance of 57 R_E (near the end of the outbound segment) the flow is mostly in the azimuthal direction with a smaller radial component.

Although viewing was not optimum, IMS also provided a direct observation of water group ion pickup near closest approach to Enceladus via a distinctive ion velocity-space distribution. In ion pickup, a newborn ion has the velocity of its parent neutral, but by virtue of its acquired electrical charge it experiences the electric field associated with the magnetospheric plasma flowing relative to the neutral-gas reference frame. The ion is accelerated by this electric field and by the ambient magnetic field such that it subsequently executes a cycloidal motion, which may be described as a circular gyration about a magnetic field line that is moving with the plasma flow velocity. In velocity space, the pickup ions exhibit a characteristic signature: a ring-shaped peak in phase space density centered on the local bulk flow velocity and with a radius equal to the flow speed at the point of ionization (Fig. 5). The ions detected by IMS are consistent with the distribution expected for pickup into plasma, flowing at 17.5 km s^{-1} with respect to the neutrals and subsequently slowing to 14 km s^{-1} at the observation point. This is well below the relative corotation-

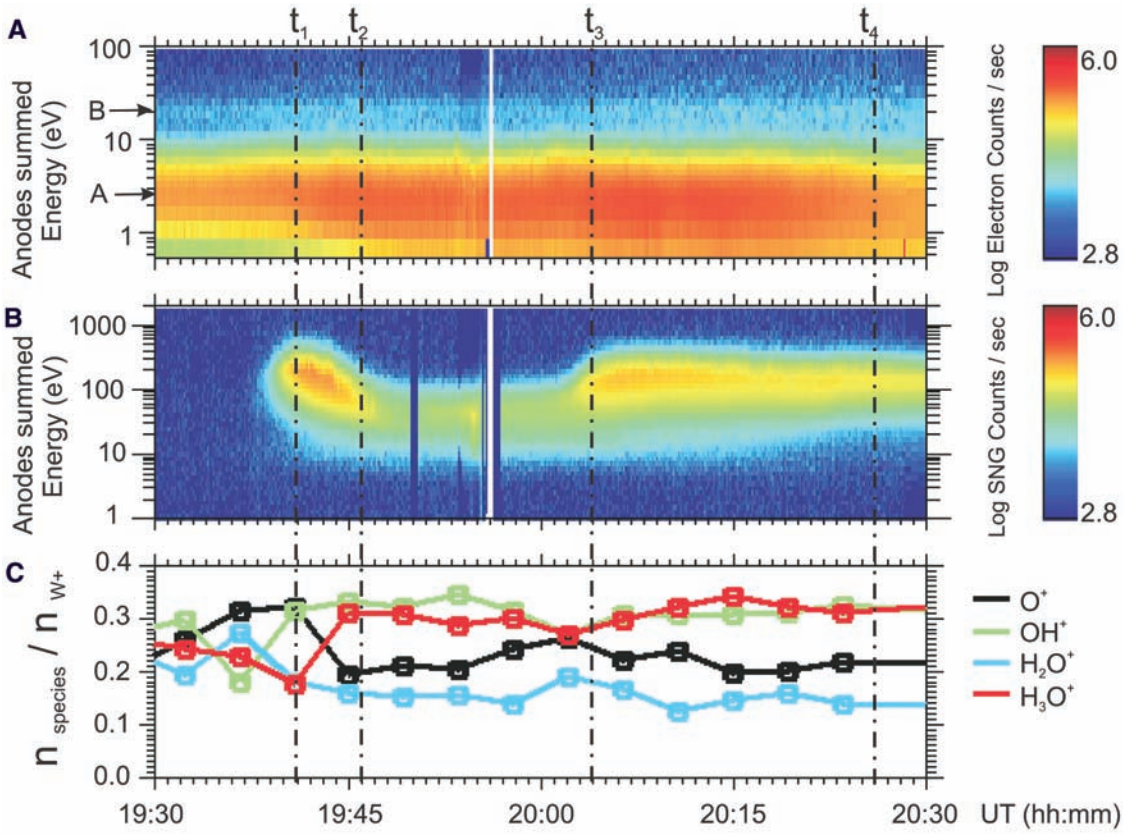

Fig. 3. Data from the CAPS on 14 July 2005. (**A**) Electron counting data from ELS. Cold and hot electron components are detected with peak counts near A and B. (**B**) Ion counting data from IMS, with the slowing of the ion flow evident between t_1 and t_2. (**C**) Individual water group (O^+, OH^+, H_2O^+, H_3O^+) ion densities divided by the total water group ion density, obtained from IMS time-of-flight measurements. The reduced χ^2 for the composition fits averages to 8.5 for O^+, 33.9 for OH^+, 8.1 for H_2O^+, and 8.0 for H_3O^+. Thus the confidence in the fits is very good for all ions except OH^+, for which it is fair. The uncertainty in the fit is dominated by the choice of model function, not statistics. The 1-σ relative uncertainties in the densities run between 2 and 3%.

al speed at Enceladus of 26.4 km s^{-1} and more characteristic of the strongly slowed and deflected flow in the near vicinity of the satellite. This distribution indicates that the ion pickup rate increases substantially near Enceladus.

The initial quantitative interpretation of the plasma flow velocity deflections (Fig. 4) uses a modified version of an electrodynamics model originally developed for Jupiter's moon Io (*8*). Compared with Io, plasma deflection at Enceladus occurs much farther from the moon, indicating an extended neutral gas cloud with mass loading distributed over a large volume. The mass-loading rate is taken to be proportional to the neutral density (*9*), assumed in the model to vary as the inverse square of distance from Enceladus. The model solutions (indicated by the green flow contours in Fig. 4) are determined by the ratio of total mass-loading rate to the Pedersen conductance assumed for Saturn's ionosphere. The latter quantity is not well constrained observationally, but scaling from the case of Jupiter (*10*) suggests a value of ~0.1 to 1 S. If we adopt the lower value, the measured flow deflections roughly imply a total mass-loading rate of ~3 × 10^{27} H_2O/s (~100 kg/s), comparable to the rate that has been independently estimated (*2*, *3*) to be required to supply the remotely observed OH cloud. A larger conductance (*11*) would imply a correspondingly larger mass-loading rate.

The RPWS data (Fig. 2) do not indicate a substantial increase in plasma density near

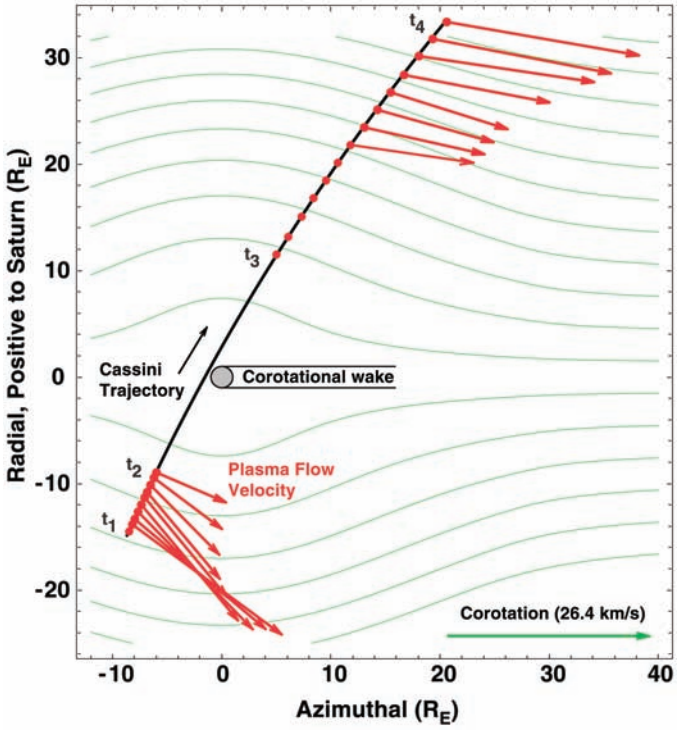

Fig. 4. Plot of the Cassini trajectory and ion flow velocities obtained from IMS (Fig. 3). IMS viewing in the radial direction is poor for about 10 min after t_3. The plasma flow is slowed and deflected over a large volume extending more than 30 R_E from Enceladus. Model streamlines (green contours) indicate a total mass-loading rate of ~100 kg s^{-1} (3 × 10^{27} H_2O molecules s^{-1}) times Σ/(0.1 S), where Σ is Saturn's ionospheric Pedersen conductance.

Enceladus, requiring that charge exchange be the dominant mass-loading process. Further support is obtained from the RPWS electron densities, ELS electron temperatures, and IMS ion flow speeds. These data indicate that the lifetime of a water molecule to electron impact ionization near Enceladus is an order of magnitude larger than the charge exchange lifetime. In addition, the ultraviolet photoionization lifetime is two orders of magnitude larger than the charge exchange

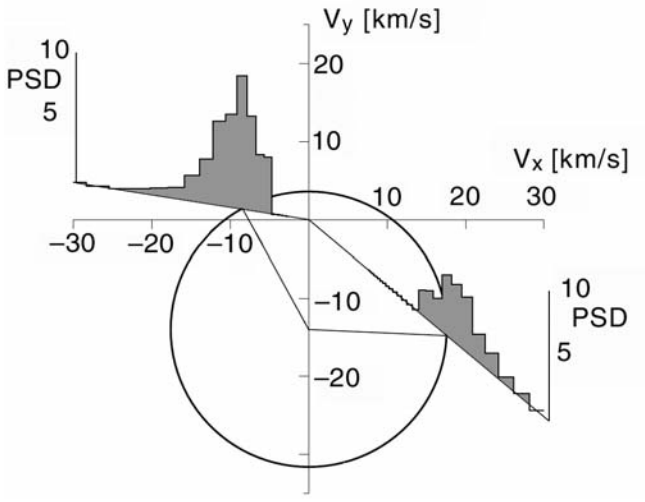

Fig. 5. Ring velocity-space distribution observed by IMS near Enceladus. The plane of the figure represents a slice through the spacecraft-centered velocity-space distribution essentially perpendicular to the magnetic field and measured 114 s before closest approach (19:53:26 UT at 4.2 R_E). The V_x direction points toward Saturn and the V_y direction is in the azimuthal direction about Saturn, positive in the westward direction. Phase space density (PSD) is in units of 10^{-6} s^3 m^{-6}. The circle shows the locus in velocity space that would be occupied by ions that were picked up in a 17.5 km s^{-1} flow that is presently flowing at 14 km/s in the $-V_y$ direction relative to Cassini. The plots on the inclined baselines show the PSD in two different directions, at gyrophase angles of ~165° and ~–45° relative to the V_x axis and at ~110° and 95° from the magnetic field direction. In both directions, the peaks in the PSD occur at a velocity consistent with the ring location as shown. This ring-type distribution constitutes direct evidence for ion pickup in the slower flows that characterize the near-Enceladus environment.

lifetime. Charge exchange is a process in which a fast ion captures an electron from a slow neutral in the vicinity of Enceladus. It produces, on average, a fast neutral and a slow ion. After such an interaction, the local ion density does not change, but the rotating fields pick up and accelerate the ion, producing the observed mass loading. The charge exchange process described here produces an enormous expansion of the Enceladus cloud by creating the energetic neutrals (*12*) that are required to describe the large-scale OH cloud observed by the Hubble Space Telescope.

References and Notes

1. D. E. Shemansky *et al.*, *Nature* **363**, 329 (1993).
2. S. Jurac *et al.*, *Geophys. Res. Lett.* **29**, 2172 (2002).
3. J. D. Richardson, S. Jurac, *Geophys. Res. Lett.* **31**, 24803 (2004).
4. D. T. Young *et al.*, *Space Sci. Rev.* **114**, 1 (2004).
5. D. A. Gurnett *et al.*, *Space Sci. Rev.* **114**, 395 (2004).
6. M. K. Dougherty *et al.*, *Science* **311**, 1406 (2006).
7. E. C. Sittler *et al.*, *Geophys. Res. Lett.* **32**, L14S07 (2005).
8. T. W. Hill, D. H. Pontius Jr., *J. Geophys. Res.* **103**, 19879 (1998).
9. J. H. Waite Jr. *et al.*, *Science* **311**, 1419 (2006).
10. D. F. Strobel, S. K. Atreya, in *Physics of the Jovian Magnetosphere*, A. J. Dessler, Ed. (Cambridge Univ. Press, New York, 1983), pp. 51–67.
11. L. E. Moore, M. Mendillo, I. C. F. Mueller-Wodarg, D. L. Murr, *Icarus* **172**, 503 (2004).
12. R. E. Johnson, M. Liu, E. C. Sittler Jr., *Geophys. Res. Lett.*, in press.

13. We wish to thank the large number of scientists and engineers on the CAPS and RPWS teams who made the results reported here possible, particularly L. K. Gilbert for help in the production of Fig. 3 and M. Dougherty of the Cassini magnetometer (MAG) team for graciously providing MAG data. The work at Los Alamos was performed under the auspices of the U.S. Department of Energy. The work of U.S. coauthors was supported by Jet Propulsion Laboratory contract 1243218 with Southwest Research Institute and contract 961152 with the University of Iowa. Work in the United Kingdom was supported by the Particle Physics and Astronomy Research Council. Cassini is managed by the Jet Propulsion Laboratory for NASA.

6 October 2005; accepted 21 November 2005
10.1126/science.1121061

REPORT

Enceladus' Varying Imprint on the Magnetosphere of Saturn

G. H. Jones,[1]* E. Roussos,[1] N. Krupp,[1] C. Paranicas,[2] J. Woch,[1] A. Lagg,[1] D. G. Mitchell,[2] S. M. Krimigis,[2] M. K. Dougherty[3]

The bombardment of Saturn's moon Enceladus by >20–kiloelectron volt magnetospheric particles causes particle flux depletions in regions magnetically connected to its orbit. Irrespective of magnetospheric activity, proton depletions are persistent, whereas electron depletions are quickly erased by magnetospheric processes. Observations of these signatures by Cassini's Magnetospheric Imaging Instrument allow remote monitoring of Enceladus' gas and dust environments. This reveals substantial outgassing variability at the moon and suggests increased dust concentrations at its Lagrange points. The characteristics of the particle depletions additionally provide key radial diffusion coefficients for energetic electrons and an independent measure of the inner magnetosphere's rotation velocity.

The importance of interactions between the Kronian magnetosphere and the Enceladus/E-ring system is becoming increasingly apparent. Saturn's inner magnetosphere is awash with ionized components of water (*1*) that probably originate at the E-ring (*2*) and, as recently confirmed, ultimately at Enceladus itself (*3*, *4*). This material substantially alters the inner Kronian magnetosphere, being analogous in several respects to the volcanic material from Io that shapes Jupiter's magnetosphere. Previous observations of the Enceladus-magnetosphere interaction region by Pioneer 11 and Voyager 2 (*5*), at 3.950 Saturn radii (R_S) from the planet (*6*), totaled four crossings of saturnian magnetic field lines that intersect Enceladus' orbit, i.e., the moon's L-shell. During July 2004 to October 2005, Cassini performed 30 such L-shell crossings, providing a wealth of information on the magnetospheric effects of the moon and the E-ring core through the Low Energy Magnetospheric Measurement System (LEMMS) (*7*) of the Magnetospheric Imaging Instrument (MIMI). LEMMS uses semiconductor detectors to measure ion and electron fluxes in the energy ranges of 20 keV to 60 MeV and 20 keV to 5 MeV, respectively, usually at a 5.65-s resolution. As well as being ion sources, Enceladus and the E-ring are important sinks for saturnian radiation-belt particles. Brown and collaborators (*8*) consider the consequences of energetic-particle bombardment for the moon's surface chemistry. Here, we report expanded observations of the reciprocal processes: Enceladus' effect on the energetic-particle population and the remote sensing of substantial variability in its outgassing rate. The latter's changing effect on energetic particles may have important implications for the inferred age of the moon's radiation-weathered surface.

Within the radiation belts, low-energy magnetospheric plasma corotates almost rigidly with Saturn (*1*). Within the LEMMS energy range, gradient and curvature drifts are pronounced: Positive ions drift azimuthally in the sense of corotation, and electrons in the opposite direction. Low-energy electrons counterdrift slowly enough to maintain a net motion in the corotation direc-

[1]Max Planck Institut für Sonnensystemforschung, Max-Planck-Str. 2, 37191 Katlenburg-Lindau, Germany. [2]Applied Physics Laboratory, The Johns Hopkins University, 11100 Johns Hopkins Road, Laurel, MD 20723–6099, USA. [3]The Blackett Laboratory, Imperial College London, London SW7 2BW, UK.

*To whom correspondence should be addressed. E-mail: jones@mps.mpg.de

The Interaction of the Atmosphere of Enceladus with Saturn's Plasma

R. L. Tokar, R. E. Johnson, T. W. Hill, D. H. Pontius, W. S. Kurth, F. J. Crary, D. T. Young, M. F. Thomsen, D. B. Reisenfeld, A. J. Coates, G. R. Lewis, E. C. Sittler and D. A. Gurnett

Science **311** (5766), 1409-1412.
DOI: 10.1126/science.1121061